Simulation of a Maize Ear Picking Device with a Longitudinal Horizontal Roller Based on Hypermesh Modeling

Jianjian Tai, Haitao Li,* Yunyi Guan, Ning Ding, Yuefeng Du, and Enrong Mao

As a key component of mechanized maize harvesting, the performance of the ear picking device directly affects the operational level of a maize harvester. Because the short harvest period of maize and the multiple experimental factors that lead to the field and bench tests cannot meet the actual research and developmental needs of manufacturing a maize harvester, this paper uses virtual prototype technology to study the influence of design and the motion parameters of a longitudinal horizontal roller in terms of picking performance. Based on the establishment of the finite element model of the corn and the ear picking device, this paper establishes evaluation indicators respectively, analyzes and evaluates the influence of the picking roller and the ground inclination angle, the picking roller speed, and the forward speed of the harvester on the performance of ear picking. Finally, a virtual orthogonal test analysis was carried out for the two factors of the picking roller speed and the forward speed of the harvester, and the significant influence of the picking roller speed and the forward speed of the harvester on the performance of the picking was compared. The research results of this paper can provide reference for optimizing the design of ear picking mechanism.

INTRODUCTION

Ear picking devices are the core of maize ear harvester headers. According to different configuration modes, they can be divided into roller ear picking devices, pulling rollers, or picking plates combined with an ear picking device (Liu *et al.* 2018). According to their different installation methods, a roller type device can be divided into three types: the longitudinal horizontal roller, the vertical roller, and the horizontal roller. Among them, the longitudinal horizontal roller structure is one of the primary types of maize harvester header used both locally and globally. The longitudinal horizontal roller harvester is a maize harvester header with one or more pairs of ear picking rollers. As the harvester moves, each row of plants, in turn, enters between the two rollers. The mutually rotating picking rollers pull the stalks downward and the maize stalk is pulled off. However, the longitudinal horizontal roller harvesting method can easily cause maize ear gnawing, with up to 30% of the total ears receiving damage. Moreover, due to the impact of the picking roller, the seeds can easily break and fall off at the root of the maize ear, resulting in a large portion of the harvest being lost, as well as a high proportion of damage (Cui *et al.* 2019).

Some scientific research institutes and universities, both local and abroad, have performed research on the biomechanical properties of maize and ear picking related injury

(Martin *et al.* 1987; Hiregoudar *et al.* 2011; Cook *et al.* 2014; Saini *et al.* 2015; Cheng *et al.* 2016; Yang *et al.* 2016; Aguayo *et al.* 2017; Fu *et al.* 2019, 2020). Balastreire *et al.* (1982) accurately measured the critical value of the fracture toughness of maize. Brass and Marley (1973) carried out experiments on the mechanical properties of maize seeds and found that the mechanical properties of different parts of seeds were different, as well as their degrees of impact force. Srivastava *et al.* (1976) studied the shear properties of maize under an impact load, and the results showed that the shear strength of maize was inversely proportional to its water content and proportional to its impact velocity. According to the compression, shear, and impact tests performed on maize kernels, Zhao *et al.* (1996) verified that the compressive and shear strength of maize kernels decreased as the water content increased. Zhou (2010) carried out experiments on the impact characteristics of maize ears, *i.e.*, its moisture content, different impact direction, and impact position. Fan *et al.* (2002) analyzed the factors affecting the rate of kernel breakage and the picking process loss percentage and obtained the experimental combination with the smallest breakage rate. Zhang *et al.* (2007) performed an experimental study on the shear fracture values of maize kernels and analyzed the shear characteristics of maize kernels under different forces and moisture contents. By combining theoretical analysis with bench test, Geng *et al.* (2016) analyzed the damage to corn in the process of ear picking, such as the gap between the picking rollers, ear diameter and ear length.

All of these studies obtained the mechanical properties of corn grains, the combination of optimum parameters, and the main factors influencing the damage resulting from ear picking by using experimental methods, but field experiments or test bench experiments could not meet the current research needs of corn ear picking mechanism. Due to the strong seasonality of maize harvests and their short harvest period, the amount of data is insufficient. If comprehensive data are needed, the time cycle is long. At the same time, due to the variety of maize species, climate differences, water contents, difference in suitable harvest periods, *etc.*, the results of field tests or bench tests cannot fully reflect the working effect of the different varieties and water contents of maize harvest processes in China. Based on the above reasons and combined with the development status of virtual prototype technology, virtual prototype technology was proposed to analyze the corn ear picking process, and the motion parameters and mechanical parameters of the corn ear during the process were obtained through simulation. The corresponding relationship between these parameters and the performance of corn picking mechanism was used to evaluate the performance of corn picking mechanism in order to provide reference for the parameter optimization of a corn picking device.

EXPERIMENTAL

Solid Modeling of the Maize Plant and Picking Roller
Physical properties and modeling of maize

According to the requirements of the GB/T 21961 (2008), the test indexes and methods were selected. The maize variety Zhengdan 958 was selected for this test. In September 2019, the plants in the maize planting experimental field of the China Agricultural University were determined to be in the full ripe stage. In the experimental area, four representative lines were selected for determination, with 10 plants in each line, and a total of 40 data groups. The measured indexes included the following: the plant natural height, ear height, ear diameter, ear length, length of the ear stalk, diameter of the

ear stalk, diameter of the root stem, and stem diameter at the ear. The measured parameters of the maize samples were sorted and counted, and the size distribution was obtained, as shown in Fig. 1.

Frequency Distribution of Plant Natural Height

a

Frequency Distribution of Ear Height

b

Frequency Distribution of Root Diameter

c

Frequency Distribution of Ear Position Diameter
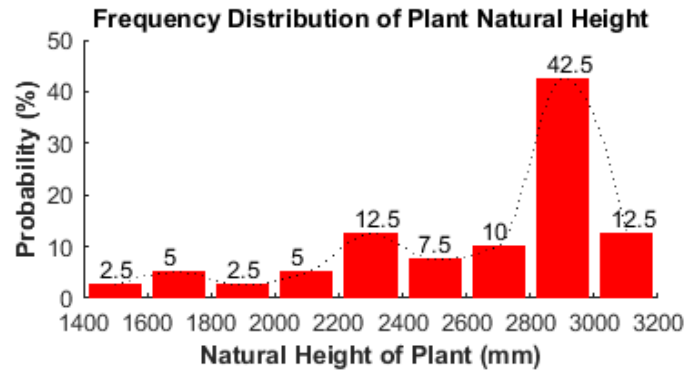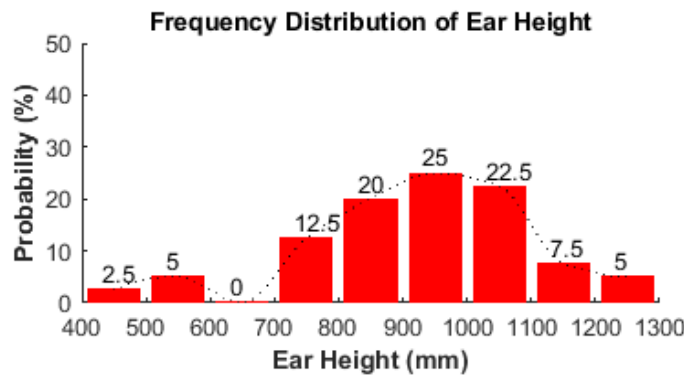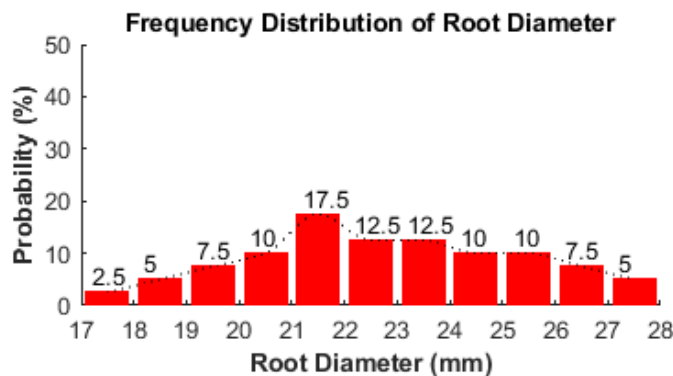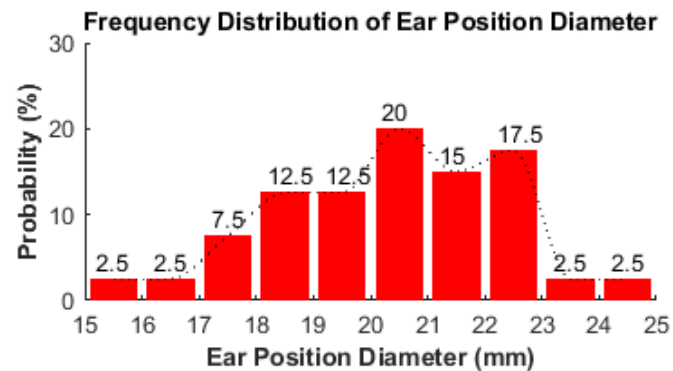
d
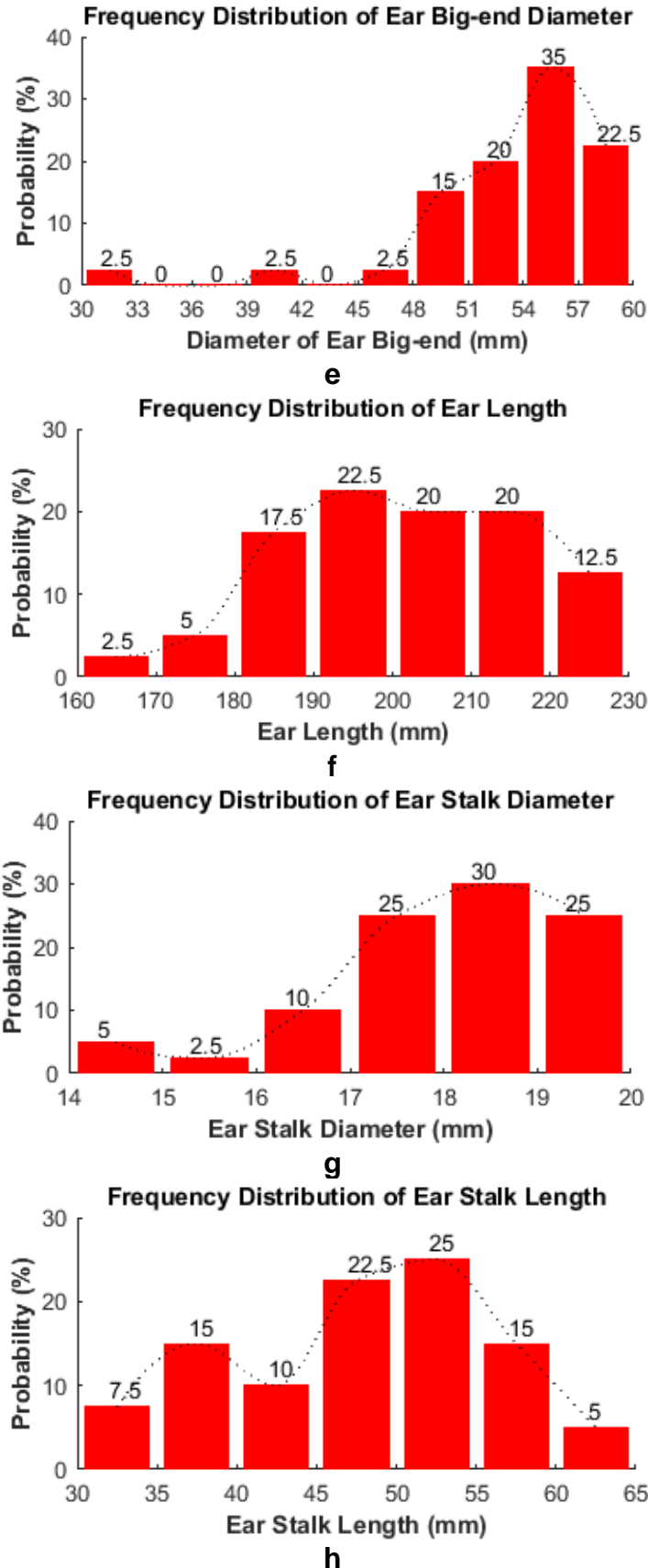
Fig. 1. Probability statistics of the maize plant size distribution measured in the field

According to the distribution of various parameters of corn plants, based on the mathematical expectation value of each parameter and combined with the distribution of its frequency, reasonable modeling parameters were selected to establish a three-dimensional solid model of corn plants. The selected parameters are shown in Table 1.

Table 1. Selection Data of Maize Plant Modeling

Item	Plant Height h (mm)	Ear Height of Maize h_0 (mm)	Root Diameter of the Plant d_0 (mm)	Diameter of Ear Position d (mm)	Diameter of Ear Big-end d_g (mm)	Ear Length l (mm)	Ear Stalk Diameter d_1 (mm)	Ear Stalk Length l_0 (mm)
Numerical value	2850	950	22	20	55	195	18	50
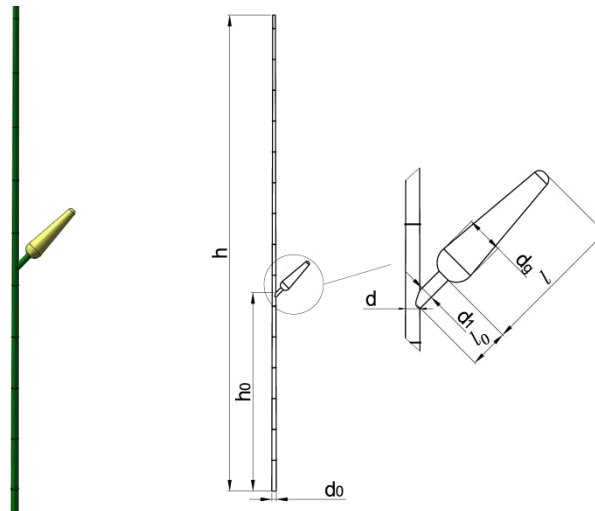
Fig. 2. Solid model of the maize plant

Because the protective effect of the maize bracts on the maize ears was not considered in the simulation process, the maize ear bracts will not appear in the simulation. In addition, since the purpose of the simulation was to obtain the force applied to the bottom of the maize ear, the force applied to each maize kernel could be approximated. Therefore, the maize ears were no longer refined, and the whole maize ear was analyzed as a whole. The simplified plant is composed of a stalk, stalk node, ear stem, and ear. According to the data in Table 1, the solid maize plant model was established using Siemens NX drawing software (version 10.0, Siemens PLM Software, Plano, Texas), as shown in Fig. 2.

Design and solid modeling of the longitudinal horizontal roller ear picking device

As shown in Fig. 3, the ear picking roller was designed according to the two following conditions: the ear picking roller can grasp the stalk and the ear picking roller cannot grasp the ear.

The diameter design of the picking roller should meet the following requirements, as stated by Eq. 1,

$$\frac{d-h}{1-\dfrac{1}{\sqrt{\mu_j^2+1}}} \leq D \leq \frac{d_g-h}{1-\dfrac{1}{\sqrt{\mu_g^2+1}}} \tag{1}$$

where h is the horizontal clearance between the two picking rollers (mm), d is the maize stalk diameter at the ear position (mm), d_g is the big-end ear (mm), μ_j is the equivalent friction coefficient of the picking roller to stalk , μ_g is the equivalent friction coefficient of the picking roller to ear, and D is the diameter of the picking roller (mm).

The horizontal clearance between the two picking rollers should meet the following requirements, as shown in Eq. 2,

$$h = 0.3d \sim 0.5d \tag{2}$$

where h is the horizontal clearance between the two picking rollers , d is the maize stalk diameter at the ear position , d_g is the big-end ear (mm), D is the diameter of the picking roller, β is the horizontal inclination angle of the pick roll, and L is the length of the pick roll.
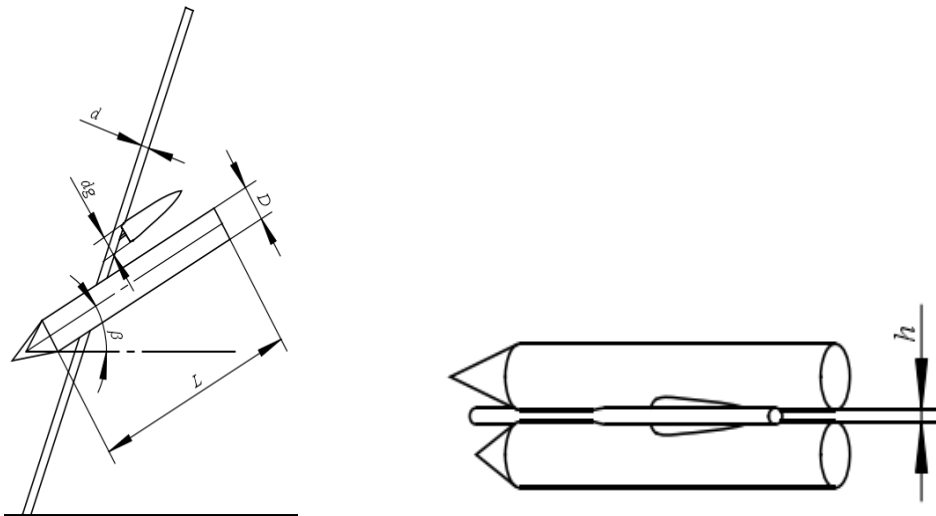
Fig. 3. Schematic diagram of the harvesting principle and structure of the picking roller

The minimum working length of the picking section should ensure that the highest and lowest ears at the ear position can be picked, as shown in Fig. 4. The L_{min} can be calculated according to Eq. 3,

$$L_{min} = L_g / \sin \beta \tag{3}$$

where β is the horizontal dip angle of the picking roller (°), and L_g is the height difference between the highest and lowest ears (mm).

According to the selected data used for the maize plant modeling, when combined with Eqs. 1, 2, and 3, the dimensions of the picking roller were determined as follows: the diameter of the picking roller was D = 70 mm; the horizontal clearance of the two picking rollers was h = 8mm; and the length of the ear picking roller was L = 700 mm.
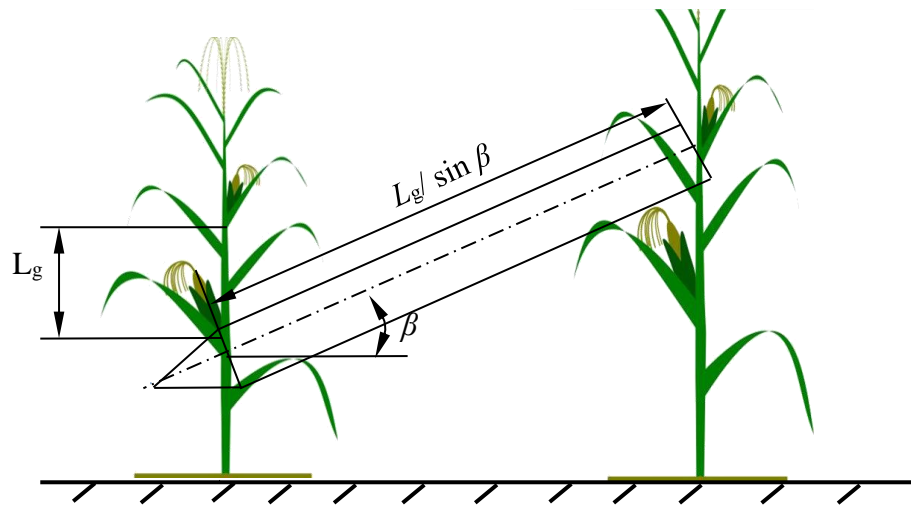
Fig. 4. Working length of the horizontal picking roller

For the actual production process, the roller ear picking mechanism is primarily composed of three parts: the ear picking roller, the reel chain, and the conveying device. Considering that the finite element model needs to reflect the real situation as much as possible, while the virtual prototype simulation test time cannot be too long, the picking mechanism model was simplified as a pair of picking rollers with spiral ribs. According to the above design data, the model of the picking roller was established using NX drawing software. The model is shown in Fig. 5.

Fig. 5. Solid model of the ear picking device

Establishment of the Finite Element Model of the Maize Plant and Ear Picking Mechanism

The 3D solid model established in NX was imported into Hyper-Mesh through the interface between Siemens NX and Hypermesh (version 12.0, Altair, Troy, MI), and the finite element model of the maize plant and ear picking mechanism was established. In the simulation analysis, a hexahedron was selected to divide the regular structural parts, and a tetrahedron was selected to divide the irregular structural parts.

Rubber materials were used for the maize stalk, maize stalk node, and maize ear, which belonged to the hyper-elastic model. Therefore, MAT_Johnson-cook was used as

the material model for the maize stalk, maize stalk node, and maize ear. At the same time, since there is no deformation of the picking roller and plate during the actual picking process, and the material itself is a rigid body, MAT_SOLID was selected as the material model of the picking roller in the simulation analysis. Under the known conditions of the material model, *i.e.*, the density, elastic modulus, and Poisson ratio, the related parameters calculated from the above parameters were defined. The basic parameters of the material properties of each component of the simulation model are shown in Table 2.

Table 2. Basic Parameters of the Material Properties of the Maize Plant and Picking Roller

Item	Density (g/cm³)	Elastic Modulus (GPa)	Poisson Ratio
Maize plant	0.9	0.06	0.33
Picking roller	7.8	120	0.3

In this paper, the lines were used to set the unit side length. The unit side length of the finite element model of the ear picking roller, maize stalk, maize ear, and maize ear stalk were set as 0.05 m, and the unit side length of the finite element model of the maize stalk node was 0.04 m. According to the topological structure of the geometric solid model in the sweeping direction, a sweeping mesh was selected. The finite element model of the maize plant and the picking roller is shown in Fig. 6.
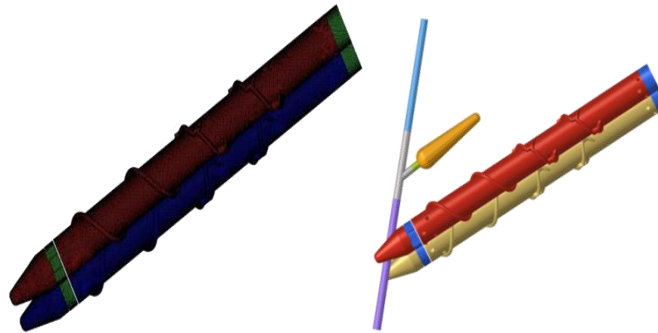
Fig. 6. Finite element model of the maize plant and ear picking roller as well as their interaction force

According to the material characteristics and related theories of the picking roller and maize plant, the contact parameter data used in the simulation model was obtained. The specific parameters are shown in Table 3.

Table 3. Contact Parameters

Item	Static Friction Coefficient (F_S)	Dynamic Friction Coefficient (F_D)	Exponential Attenuation Coefficient (D_C)	Viscous Friction Coefficient (V_{FC})	Viscous Contact Damping (V_{DC})
Maize stalk and picking roller	0.89	0.728	0.001	0.0	30
Maize ear and picking roller	0.75	0.645	0.001	0.0	30

bioresources.com

Simulation Analysis Based on the Finite Element Model

The forward speed of the harvester was set as 1.5 m/s, and the rotational speed was 1000 rpm. Before entering the picking device, the maize plant will tilt forward due to the feeding action of the reel chain. For this picking device, the maize plant is inclined towards the direction of picking device at a 10° angle. The dip angle between the picking roller and the ground was selected as simulation variable, and the tested dip angles ranged from 28° to 36° with a total of 9 groups of tests. The stress on the bottom of the ear caused by the dip angle between the picking device and the horizontal ground was studied. Through virtual simulation, the contact forces of the 18 selected points under 9 working conditions were obtained, as shown in Table 4. According to statistics, the maximum and absolute values of forces on the bottom of corn ear at different dip angles are shown in Table 5.

Table 4. Force Statistics of 18 Units at the Moment of Ear Picking
Unit: N

Unit No Dip Angle(°)	28	29	30	31	32	33	34	35	36
31187	1704	1222	4	3	116	1553	1366	4533	4763
30761	41	1377	1882	589	249	386	530	736	2
30035	3045	1030	193	183	1647	5	3398	72	7
29909	5	322	19	3	7	3	4	72	385
29226	2	202	144	5	37	488	610	2	661
28800	605	251	29	5	3	374	344	187	4102
30336	4206	738	609	98	6	4	255	602	3
30762	341	393	41	703	1067	17	417	1233	4
31188	1132	2899	8	3	221	738	546	2025	176
28801	631	239	373	125	1	541	1297	664	4942
29227	6	37	319	119	1401	198	1114	2	826
29908	6	379	19	3	154	1	219	80	454
30334	785	899	83	8	353	274	1003	3192	80
30760	18	1292	1778	8	42	189	172	1047	0
31186	277	781	3	4	14	1713	826	1113	2417
31612	1805	1671	3	44	125	253	3134	1300	2014
29910	2	349	2	2	1	19	2	3	724
29225	148	502	2	1	2	253	188	42	415

Table 5. Statistics of the Maximum Force and Absolute Value of Different Inclinations

Project	28	29	30	31	32	33	34	35	36
Maximum force (N)	4206	2899	1882	589	1647	1713	3398	4533	4942
Absolute value sum of forces (N)	14759	14583	5511	1906	5446	7009	15423	16905	21975
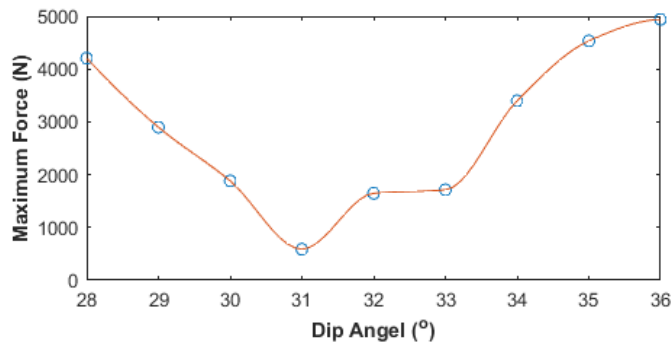
Fig. 7. The relation between the maximum force on selected element and dip angle
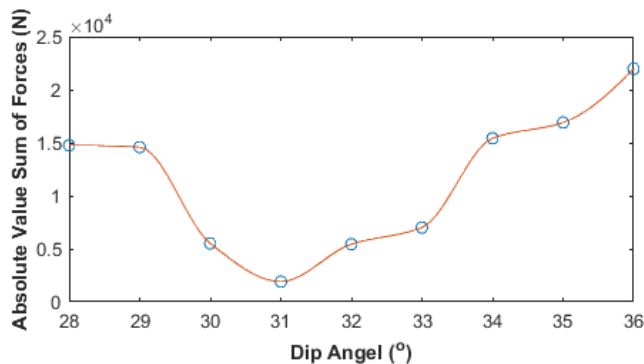
Fig. 8. The relation between absolute force value and dip angle of selected element

It can be seen in Table 5 that when the dip angle between the picking roller and the ground is 28° to 31°, as the dip angle increases, the total contact force on all units as well as the maximum force on the unit are predicted to gradually decrease. When the dip angle between the picking roller and the ground is 31°, the total contact force of all the units is at its minimum, and the maximum force of the unit is also at its minimum. When the angle between the picking roller and the ground is 31° to 36°, the total contact force on all units and the maximum force on the unit gradually increase. As the dip angle is changed, the trends of the total force and maximum force of the selected elements are shown in Figs. 8 and 9. The above simulation shows that, when the inclination angle is small, the contact time between the picking roller and the ear is relatively long, which leads to more stress points at the bottom of the ear of corn and longer time. When the angle of inclination is too large, the impact force of the picking roller on the ears will increase, causing gnawing injuries to the bottom of the ears and part of the grains falling to the field ground, resulting in harvest loss.

It can be seen in Tables 4 and 5 that the contact force of the picking roller with

spiral ribs is relatively concentrated, which makes the force on the ear uneven and yields a large force difference at each position. This is also the primary reason for ear gnawing and kernel breakage. Therefore, measures such as increasing the diameter of the picking roller, reducing the height of the spiral rib, improving the smoothness of the picking roller, and spraying plastic on the surface of picking roller can effectively reduce the maize kernel breakage rate and ear damage rate.

Effect of the Rotational Speed on the Ear Harvesting Force and Harvesting Time

The forward speed of the harvester was set as 1.8 m/s, and the angle between the picking roller and the ground was 30°. Before entering the picking device, the posture will tilt forward due to the feeding action of the reel chain. For this picking device, the maize plant is inclined towards the direction of picking device at a 10° angle. For this test, rotational speed was set to 800 rpm, 900 rpm, 1000 rpm, 1100 rpm, and 1200 rpm as the simulation variable. The effect of the rotational speed on the stress at the bottom of ear and picking time were studied. Through virtual simulation, the curve of the maximum contact force and picking time of the ear in the picking mechanism for five working conditions were obtained, as shown in Fig. 9.
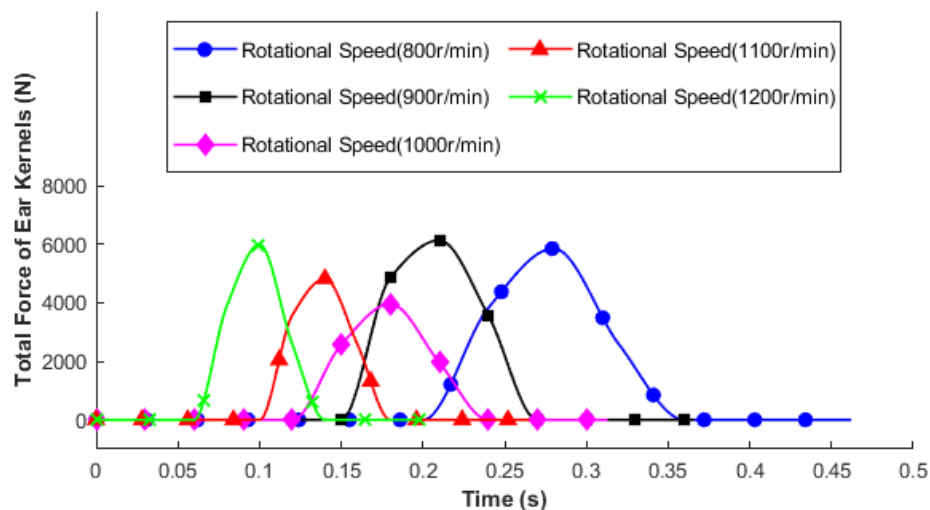
Fig. 9. The ear contact force and the picking time at different rotational speed

It can be seen in Fig. 9 that as the rotational speed increases, the sum of the instantaneous maximum contact force between the bottom of the ear and the picking roller gradually increases, and the time gradually decreases. The total force of the 18 selected points fluctuated from 3956 N to 6128 N; the average stress of each point increased by 220 N to 340 N, and the overall picking time gradually decreased by 0.198 s to 0.462 s. These results were caused by the increase of the speed, which can be explained according to the momentum theorem. The increment of momentum of an object is equal to the impulse of the combined external force. The impact force is directly proportional to the impact velocity and inversely proportional to the impact time. When the rotational speed increases, the vertical speed of the maize stalk gradually increases, and the required picking time decreases. Thus, the contact force between the ear and the picking roller will gradually increase.

Combined with the actual process of picking, it can be seen that increasing the

bioresources.com

rotational speed can improve the efficiency of the ear picking process. At the same time, it will also cause greater damage to the kernels, especially when the moisture content of the kernels is relatively high. According to the mechanical properties of a kernel, the maximum extrusion and impact force that the kernel can bear is approximately 300 N to 500 N. When the rotational speed is too high, the protection provided by the bracts on the kernel is limited, which will inevitably cause cracks in the kernel or for it drop directly.

Effect of the Forward Speed of the Harvester on the Ear Harvesting Force

The rotational speed was set to 1000 rpm, and the dip angle between the picking roller and ground was 30°. The plant tilted at a 10° angle to the picking device before entering the picking device. For this test, the speed of the picking roller was set to 0.9 m/s, 1.2 m/s, 1.5 m/s, 1.8 m/s and 2.1 m/s as the simulation variable. The effect of the rotational speed on the stress at the bottom of the ear and the picking time were studied.

The curve of the force situation and picking time of the ear in the picking mechanism for five working conditions were obtained, as shown in Fig. 10.
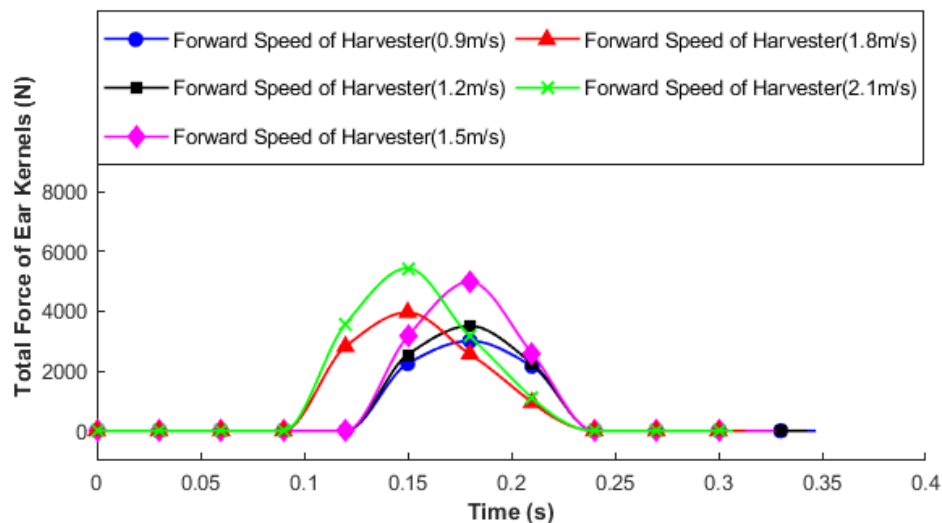
Fig. 10. The ear contact force and the picking time at different forward speeds of the harvester

It can be seen in Fig. 10 that as the forward speed increases, the sum of the instantaneous maximum contact force between the ear bottom and the picking roller fluctuates between 3006 N and 5433 N, and the average stress at each point ranges from 167 N to 302 N, but the overall trend gradually increases. Meanwhile, as the forward speed is increased, the picking time is decreased by 0.347s to 0.307s. The reason for this is that the inertia in the forward direction increases and the impact force of the ear increases with an increase of the working speed, which leads to an increase of the instantaneous contact force between the ear and the picking roller. Thus, the picking time was reduced.

Virtual Orthogonal Experiment of the Picking Process

Taking the rotational speed and the forward speed of the harvester as the experimental factors, and taking the contact force between the ear and the picking roller as well as the picking time as the response values, the orthogonal experiment was conducted at two factor levels. The factors and coding levels of the virtual orthogonal test are shown in Table 6.

bioresources.com

Table 6. Factor Levels of the Virtual Orthogonal Test

Coding Level	Factor A: Speed of the Picking Roller (r/min)	Factor B: Forward Speed of the Harvester (m/s)
-2	800	0.9
-1	900	1.2
0	1000	1.5
1	1100	1.8
2	1200	2.1

Through virtual experiment simulation, the results are shown in Table 7. The orthogonal experimental design model combination test was carried out for the rotational speed and the harvester operation speed at the coding levels shown in Table 7. The results showed that the collision force between the ear and the picking roller ranged from 2821 N to 7440 N, with an average force of 156.72 N to 413.00 N, while the picking time ranged from 0.148 s to 0.572 s.

Table 7. Results of the Virtual Orthogonal Test

Test No.	Factor a:Rotational speed (r/min)	Factor b: Forward Speed of the Harvester (m/s)	Contact Force Between the Ear and the Picking Roller Y_1 (N)	Picking Time Y_2 (s)
1	-2	-2	6202	0.572
2	-1	-2	6180	0.492
3	0	-2	3006	0.463
4	1	-2	2821	0.462
5	2	-2	5675	0.461
6	-2	-1	6538	0.416
7	-1	-1	6157	0.413
8	0	-1	3502	0.412
9	1	-1	5427	0.366
10	2	-1	6523	0.350
11	-2	0	6127	0.347
12	-1	0	5964	0.343
13	0	0	4982	0.327
14	1	0	6329	0.313
15	2	0	7440	0.307
16	-2	1	5848	0.287
17	-1	1	6127	0.277
18	0	1	3956	0.274
19	1	1	4818	0.265
20	2	1	5988	0.232
21	-2	2	6304	0.219
22	-1	2	6157	0.202
23	0	2	5433	0.200
24	1	2	5202	0.198
25	2	2	5608	0.148

Using MATLAB software (2017bversion, MathWorks, Natick, MA), the response surface analysis experiments were performed with the rotational speed (a) and the working speed (*b*) of the harvester as the experimental factors, and the contact force (Y_1) and the picking time (Y_2) of the ear and picking roller as the response values. The regression equation of the ear contact force (Y_1) expressed by the coding value is shown in Eq. 4,

$$Y_1 = -78814.697 + 370.288a - 46771.492b + 124.428ab - 0.509a^2 - 8972.539b^2 - 0.04a^2b - 14.057ab^2 + 4716.049b^3 \qquad (4)$$

where *a* is the rotational speed (rpm), and *b* is the speed of the harvester (m/s). According to the regression equation shown in Eq. 4, the response surface diagram of the rotational speed (a) and the forward speed (b) of the harvester with the contact force is shown in Fig. 11.
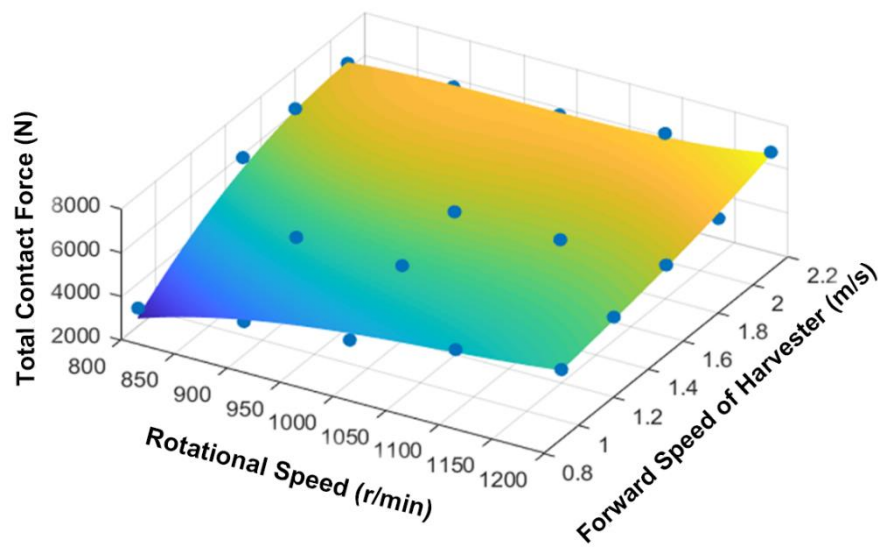
Fig. 11. Effect of the rotational speed and the working speed of the harvester on the contact force

When the rotational speed is fixed at a certain level, the contact force tends to swing with the increase of the machine speed, *i.e.*, the contact force gradually increases as the speed increases, and there is a minimum value in the middle. The overall change in value is not obvious. From the partial regression analysis, it can be concluded that the impact of the rotational speed on the contact force is greater than the effect of the forward working speed of the harvester.

The regression equation of picking time (Y_2) expressed by experimental data is shown in Eq. 5,

$$Y_2 = 5.211 - 0.009a - 3.193b + 0.003ab + 0.925b^2 - 0.148b^3 ......(5)$$

where a is the picking roller speed (rpm), and b is the speed of the harvester (m/s).

Figure 12 shows the contour map of the rotational speed and the working speed of the harvester in terms of the picking time. It can be concluded from Fig. 11 that under the conditions of a certain forward speed of the harvester, the picking time gradually decreases as the picking roller speed increases, which basically presents a linear relationship. When the rotational speed is stable at a certain level, the working speed of the harvester has a

linear relationship with the picking time, *i.e.*, the picking time decreases as the forward speed of the harvester increases. However, the response diagram and the partial return analysis show that the impact of the speed of the rotational speed on the picking time is greater than the impact of the operating speed of the harvester.
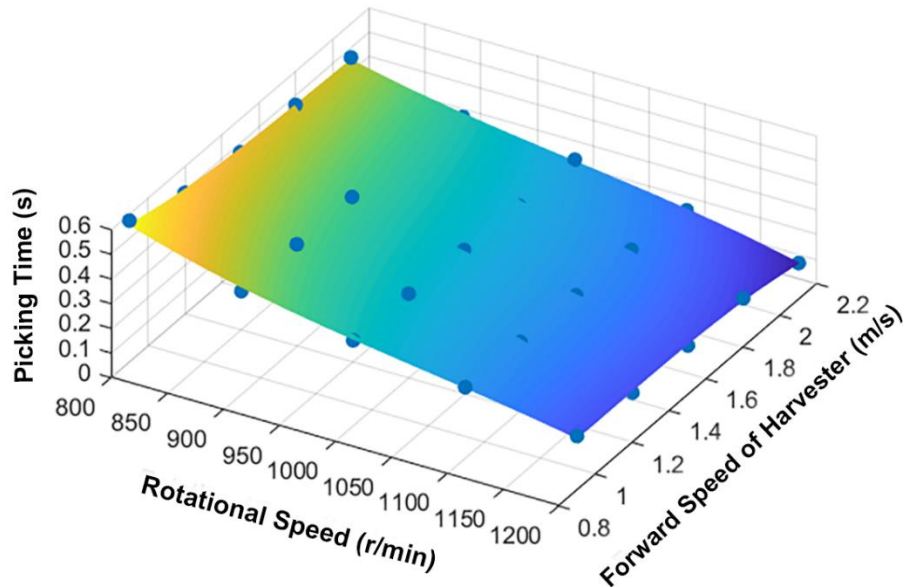
Fig. 12. Effect of the rotational speed and the forward speed of the harvester on the picking time

CONCLUSIONS

1. Based on the field measurements and statistics, the mechanical and physical parameters of a maize plant were obtained, and the maize plant modeling method for simulation was summarized. At the same time, based on the mechanical and physical parameters of the maize plant as well as the design experience, the key design parameters of the ear picking device were designed, and a solid model of the ear picking mechanism was established.

2. Based on virtual prototype technology and the force and motion analysis of a maize plant undergoing the ear picking process, the simulation method of the key components of a maize harvester was proposed. Based on the geometric structure parameters and material characteristic parameters of the primary working parts of the maize plant and ear picking mechanism, a solid model of the maize plant and picking device was imported into Hyper-Mesh software, and a finite element model of the interaction of the ear picking process was established.

3. Based on virtual prototype technology and the force and motion analysis of a maize plant undergoing the ear picking process, a method to evaluate the harvesting performance of a maize harvester with a longitudinal horizontal roll was proposed. Taking the contact force between the ears and the picking roller as the evaluation index, the influence of different dip angles between the picking roller and the ground on the picking performance was simulated. Taking the contact force between the ear and

bioresources.com

picking roller, as well as the picking time, as the evaluation indexes, the primary virtual simulation experiments were carried out to analyze the influence of two factors, *i.e.*, the different rotational speed and the different harvester operating speeds, on the performance of the ear picking process. Meanwhile, a virtual orthogonal experiment was carried out to analyze two factors, *i.e.*, the rotational speed and the forward speed of the harvester, and their influence on the picking performance was compared.

ACKNOWLEDGMENTS

REFERENCES CITED

Aguayo, M. M., Sarin, S. C., Cundiff, J. S., Comer, K., and Clark, T. (2017). "A maize-stover harvest scheduling problem arising in cellulosic ethanol production," *Biomass and Bioenergy* 107, 102-112. DOI: 10.1016/j.biombioe.2017.09.013

Balastreire, L. A., Herum, F. L., and Blaisdell, J. L. (1982). "Fracture of maize endosperm in bending part II: Fracture analysis by fractography and optical microscopy," *Transactions of the ASABE* 25(4), 1062-1065. DOI: 10.13031/2013.33668

Brass, R. W., and Marley, S. J. (1973). "Low damage maize shelling cylinder," *Transaction of the ASAE* 5(2), 278-283. DOI: 10.13031/2013.37445

Cheng, X., Jia, X., Chen, M., and Li, Q. (2016). "Experiment and analysis on test device of maize ear picking by pulling stalk upwards," *Transactions of the Chinese Society of Agricultural Engineering* 32(22), 50-55.

Cook, D. E., Shinners, K. J., Weimer, P. J., and Muck, R. E. (2014). "High dry matter whole-plant maize as a biomass feedstock," *Biomass and Bioenergy* 64, 230-236. DOI: 10.1016/j.biombioe.2014.02.026

Cui, T., Fan, C., Zhang, D., Yang, L., Li, Y., and Zhao, H. (2019). "Analysis on research progress of mechanized maize harvesting technology," *Transactions of The Chinese Society of Agricultural Machinery* 50(12), 1-13.

Fan, G., Wang, H., Ji, J., Cao, W., Liu, H., Hao, J., Chen, D., Zhou, Z., and Wang S. (2002). "Analysis of influence factor on seed damage rate and loss rate during picking maize-cob," *Transactions of the Chinese Society of Agricultural Engineering* 18(4), 72-74.

Fu, Q., Fu, J., Chen, Z., and Ren, L. (2020). "Loss reduction mechanism and experiment on snapping of rigid-flexible coupling maize head," *Transactions of the Chinese Society of Agricultural Machinery* 51(4), 60-68.

Fu, Q., Fu, J., Chen, Z., Zhang, L., and Ren, L. (2019). "Influence of different maize ear position and orientation and water content on fracture mechanics of maize peduncle," *Transactions of the Chinese Society of Agricultural Engineering* 35(16), 60-69.

GB/T 21961 (2008). "Technical requirements for maize combine harvest," Standardization Administration of China, Beijing, China.

Geng, A., Yang, J., Zhang, J., Zhang, Z., Yang, Q., and Li, R. (2016). "Influence factor analysis of mechanical damage on maize ear picking," *Transactions of the Chinese Society of Agricultural Engineering* 32(22), 56-62.

Hiregoudar, S., Udhaykumar, R., Ramappa, K. T., Shreshta, B., Meda, V., and Anantachar, M. (2011). "Artificial neural network for assessment of grain losses for paddy combine harvester a novel approach," in: *Proceedings of the International Conference on Logic, Information, Control and Computation*, 25-27 February, Gandhigram, India, pp. 221-231.

Liu, C., Huang, Y., Wang, Z., Tai, Y., Liu, L., Sun, C., and Liu, H. (2018). "Emergy analysis for transportation fuels produced from maize stover in China," *Journal of Cleaner Production* 174, 213-225. DOI: 10.1016/j.jclepro.2017.10.306

Martin, C. R., Converse, H. H., Czuchajowska, Z., Lai, F. S., and Pomeranz, Y. (1987). "Breakage susceptibility and hardness of maize kernels of various sizes and shapes," *Applied Engineering in Agriculture* 3(1), 104-113. DOI: 10.13031/2013.26655

Saini, J. K., Saini, R., and Tewari, L. (2015). "Lignocellulosic agriculture wastes as biomass feedstocks for second-generation bioethanol production: Concepts and recent developments," *3 Biotech* 5(4), 337-353. DOI: 10.1007/s13205-014-0246-5

Srivastava, A. K., Herum, F. L., and Stevens, K. K. (1976). "Impact parameters related to physical damage to maize kernel," *Transactions of the ASABE* 19(6), 1147-1151. DOI: 10.13031/2013.36191

Yang, L., Cui, T., Qu, Z., Li, K., Yin, X., Han, D., Yan, B., Zhao, D., and Zhang, D. (2016). "Development and application of mechanized maize harvesters," *International Journal of Agricultural and Biological Engineering* 9(3), 15-28. DOI: 10.3965/j.ijabe.20160903.2380

Zhang, Y., Gao, L., Liu, H., and Li, X. (2007). "Experimental study on maize kernel shear crash," *Journal of Agricultural Mechanization Research* 5, 136-138.

Zhao, X., Ma, Z., Sun, Y., and Wu, W. (1996). "Experimental study on mechanical properties of maize kernels," *Journal of Jilin Agricultural University* 26(1), 60-66.

Zhou, Q. (2010). "Experimental study on impact characteristics of corn ear," *Agricultural Science and Technology & Equipment* 4, 34-35.